

Voltage-Controlled Electron-Hole Interaction in a Single Quantum Dot

A. Högele,¹ S. Seidl,¹ M. Kroner,¹ K. Karrai,¹ R. J. Warburton,² M. Atatüre,³
J. Dreiser,³ A. Imamoglu,³ B. D. Gerardot,⁴ and P. M. Petroff⁴

Received 20 August 2004; accepted 29 September 2004

The ground state of neutral and negatively charged excitons confined to a single self-assembled InGaAs quantum dot is probed in a direct absorption experiment by high resolution laser spectroscopy. We show how the anisotropic electron-hole exchange interaction depends on the exciton charge and demonstrate how the interaction can be switched on and off with a small dc voltage. Furthermore, we report polarization sensitive analysis of the excitonic interband transition in a single quantum dot as a function of charge with and without magnetic field.

KEY WORDS: quantum dot; absorption; charged exciton; electron-hole exchange; fine structure.

Spin control and manipulation in mesoscopic semiconductor systems have attracted extensive attention within the last few years. The activity in this field is driven by the idea of using spin states for quantum information processing and quantum communication. In particular, semiconductor quantum dots (QDs) have been considered for realization of spin quantum bits [1,2] as they offer the potential advantage of scalability and tunability. For spin qubit processing in QDs, an optical scheme has been envisioned [3]. Other proposals involve a combination of spin and charge excitation [4] or an all-optical implementation of quantum information processing [5] in QDs. All proposals have a common crucial requirement, namely resonant and spin selective excitation.

Significant progress has been made with naturally formed QDs [6] based on resonant control of

excitonic states [7,8], leading to the recent demonstration of an optical CROT gate [9]. Self-assembled QDs have the advantage of longer excitonic coherence time due to stronger confinement. They have been proved to serve as a source of nonclassical light for secure quantum communication [10–13]. An implementation of self-assembled QDs as a spin sensitive postprocessing read-out tool can be envisioned. Electric dipole transitions are spin sensitive, such that the spin information of the optically active state is imprinted onto the photon polarization. High efficiency single photon devices [14] could provide high yield for spin qubit detection.

Recently, we have reported resonant exciton creation into the ground state [15,16] and the first excited state [17] of a single self-assembled QD. In the work presented here, we address the topic of polarization selective resonant creation of excitonic states in a single self-assembled InGaAs QD by high resolution laser spectroscopy. We report results on the spin-mediated anisotropic electron-hole exchange and on the polarization dependence of the excitonic states as function of charge, electric, and magnetic field.

The InGaAs QDs investigated in the experiments were grown by molecular beam epitaxy in the self-assembly Stranski–Krastanow mode and

¹Center for NanoScience and Department für Physik, Ludwig-Maximilians-Universität, Geschwister-Scholl-Platz 1, 80539 München, Germany; e-mail: hoegele@lmu.de.

²School of Engineering and Physical Sciences, Heriot-Watt University, Edinburgh EH14 4AS, United Kingdom.

³Institute of Quantum Electronics, ETH Hönggerberg HPT G12, CH-8093, Zürich, Switzerland.

⁴Materials Department, University of California, Santa Barbara, California 93106, USA.

are embedded in a field-effect heterostructure [18]. Highly n -doped GaAs acts as back electrode followed by a tunnel barrier of 25 nm GaAs and the InGaAs QDs. An annealing step was introduced in order to shift the photoluminescence (PL) emission energy to around 1.3 eV [19]. The QDs are sequentially capped with 30 nm GaAs and a 120 nm AlAs/GaAs superlattice. A semitransparent NiCr gate electrode evaporated on the surface allows us to control the excitonic properties of QDs by applying a voltage with respect to the back contact. The exciton energy can be fine-tuned using gate voltage induced vertical Stark effect [17]. Furthermore, the QDs can be charged sequentially with electrons from the metallic-like back electron reservoir. For a single QD the charge state is unambiguously identified by monitoring pronounced Coulomb blockade in the PL [20,21].

We used a home-built fiber-based confocal microscope for both the PL and the differential transmission spectroscopy (Fig. 1a). For all experiments presented here, the microscope was cooled to liquid Helium temperature in a bath cryostat. Details of the experimental setup have been discussed

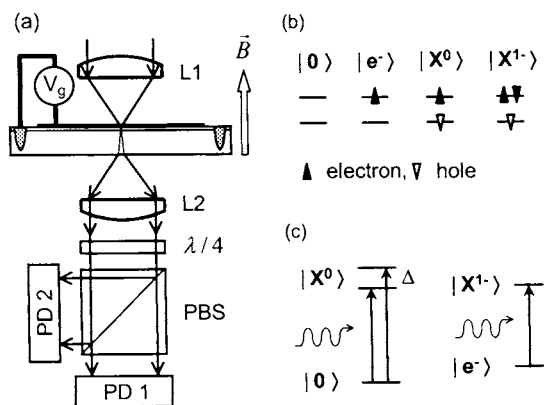


Fig. 1. (a) Optical transmission setup: Tunable narrow band laser light is delivered with an optical fiber (not shown), collimated and then focussed with the aspherical lens L1 with numerical aperture 0.55 onto the sample. The transmitted light is collimated with the lens L2. Before detection with the Ge p - i - n photodiodes (PD 1, PD 2), the transmitted light passes a quarter-wave plate ($\lambda/4$) and a polarizing beamsplitter (PBS). The charge state of quantum dots is defined by gate voltage V_g , the magnetic field B is applied in Faraday configuration perpendicular to the sample surface. (b) Quantum mechanical states in a single quantum dot: $|0\rangle$ is the vacuum state, $|e^- \rangle$ the single electron state, $|X^0\rangle$ the neutral exciton state, and $|X^{1-}\rangle$ the singly charged exciton state. (c) The level diagrams for the optical creation of a neutral exciton and a singly charged exciton. The neutral exciton is split by Δ through the anisotropic electron-hole exchange interaction.

elsewhere [15]. Excitation laser light was provided through a single-mode glass fiber, collimated and focused on the sample surface with a lens L1 with numerical aperture of 0.55. The sample was brought into the focal plane with a low temperature compatible XYZ-positioning stage (Atto Cube Systems, ANP-XYZ-100), allowing for precise vertical and lateral positioning. For most experiments, a commercial Ge photodiode was sandwiched between the sample and the positioning stage in order to detect the total laser light transmitted through the sample. Two types of Ge infrared photodetectors were used: FDG05, Thorlabs Inc. and J16-SC, EG&G Judson (J16-C11-R02M-SC) with an active diameter of 5 and 2 mm, respectively. The advantage of the latter photodiode is a factor of 5 lower noise and a factor of 3 higher bandwidth at 4.2 K. Alternatively, the photodetector was replaced by a polarization analysis setup. It is well known that fiber bending can modify the light polarization. However, by adjusting the degree of polarization with a combination of half- and quarter-wave plates before coupling the laser light into the microscope fiber, any fiber polarization contribution can be compensated. Alternatively, fiber bending paddles could be used for polarization control. The light reflected from the sample surface and detected outside the cryostat would then provide information on the degree of polarization. In our experiments however, we used the polarization analysis setup as shown in Fig. 1a in order to identify unambiguously the polarization state of the light focused onto the sample.

The polarization analysis setup contains an additional lens L2 (Geltech Aspheric Lens, 350230-B) which collimates the laser light. The parallel beam passes a quarter-wave plate (CVI, QWPO-950-04-4) with the fast axis oriented with an angle of -45° with respect to the p -axis of the polarizing cube beamsplitter PBS (CVI, PBS-930-020). The magnetic field is aligned parallel to the sample growth direction and antiparallel to the propagation k -vector of the excitation beam (Fig. 1). Given this orientation, the quarter-wave plate transforms σ^- and σ^+ circular light into linearly s -polarized and p -polarized light, respectively. The p -polarized component is transmitted onto a Ge p - i - n photodiode PD 1 (J16-C11-R02M-SC, EG&G Judson) whereas the s -component is directed to the photodiode PD 2 of the same type. The signal intensity detected by the photodiodes is anticorrelated and sums up to the total signal of the transmitted light. In order to avoid losses, the parameters of the lens L2 were chosen such that the waist of the collimated beam does not exceed the active

area of the photodetectors. The ratio of the signals on PD 1 and PD 2 allows for a direct determination of the degree of ellipticity of the excitation light. In particular, in the case of pure right-hand circular polarization, the detector PD 1 shows maximum signal whereas the signal on PD 2 is minimal. For left-hand circular polarization, the situation is reversed with minimal signal on PD 1 and maximal signal on PD 2. In order to analyze linear polarization, the quarter-wave plate had to be removed. Prior to application in the spectroscopy experiments, we tested the polarization analysis setup and we confirmed that it operated at room temperature as well as at liquid Nitrogen and liquid Helium temperatures.

Figure 1b shows schematically the quantum mechanical states in a single QD probed by means of both resonant and nonresonant spectroscopy. With nonresonant PL spectroscopy, we first identify the exciton energies and the gate voltage regions of the neutral exciton X^0 and the charged exciton X^{1-} in a single QD [20]. As observed in PL on several dozens QDs emitting around 1.3 eV, the typical corresponding voltage intervals for low excitation power are $[-0.8 \text{ V}, -0.4 \text{ V}]$ and $[-0.4 \text{ V}, -0.1 \text{ V}]$ for the X^0 exciton and the X^{1-} exciton, respectively. Then, a narrow band tunable diode laser (Sacher Lasertechnik, TEC500, $\Delta\nu \leq 5 \text{ MHz}$) is adjusted to match the energy of the interband optical transition into the neutral or singly charged excitonic ground state of the selected QD (Fig. 1c). The detuning of the transition energy with respect to the laser excitation energy is achieved through the Stark effect by sweeping the gate voltage [17]. The Stark shift depends quadratically on the applied voltage [22] but in a small range of gate voltage it can be approximated by a linear function. In the present case, the typical Stark shift is $\sim 1 \text{ meV/V}$ and does not depend on the charge state of the exciton.

Differential transmission spectra within the corresponding gate voltage interval of the neutral and charged exciton in a single QD at zero magnetic field are shown in Fig. 2. The X^0 transition, resonant with excitation laser energy $E_0 = 1.272 \text{ eV}$, exhibits two lines split by the fine structure $\Delta = 27 \mu\text{eV}$. In contrast, the X^{1-} exhibits only a single resonance. The linewidths of the resonances in Fig. 2 are 3.5 and $7.1 \mu\text{eV}$ for the π_x and π_y transition of the neutral exciton and $4.2 \mu\text{eV}$ for the X^{1-} transition. It is not always the case that the π_y resonance is broader than the π_x resonance. From time resolved measurements on single QDs in a similar sample we expect the linewidth to be $\sim 1 \mu\text{eV}$ for neutral and charged ex-

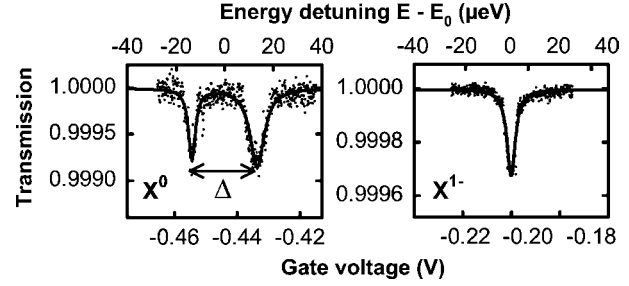


Fig. 2. Differential transmission of the neutral X^0 (left) and charged exciton X^{1-} (right) in a single self-assembled quantum dot. The detuning was achieved at constant laser wavelength by sweeping the gate voltage. The two resonances of the neutral exciton are split by the fine structure $\Delta = 27 \mu\text{eV}$. The resonance energy E_0 of X^0 was 1.272 eV and that of X^{1-} was 1.266 eV . The sample was at 4.2 K , no magnetic field was applied.

citons. However, we find that the exciton energy experiences spectral fluctuation of several microelectronvolts which broadens the resonance line [16].

The interband transition energy of the charged exciton in Fig. 2 is 6 meV below the X^0 energy, a consequence of the difference in binding energy [20]. The fine structure arises through electron-hole exchange interaction in a QD potential with reduced symmetry [23]. A splitting of several μeV is expected even for cylindrically symmetric QDs due to the lack of inversion symmetry in the underlying lattice [24]. For $\text{In}_x\text{Ga}_{1-x}\text{As}$ QDs, the splitting can be as high as $200 \mu\text{eV}$ for strongly asymmetric dots [25]; Langbein *et al.* report a decrease of the fine structure splitting down to $6 \mu\text{eV}$ with annealing [26]. In our sample, the value of the splitting varies from 11 to $42 \mu\text{eV}$ as measured on several individual QDs. The magnitude of Δ indicates that the dominant contribution arises through QD shape anisotropy. We are able to switch off the spin mediated electron-hole exchange by applying a small dc voltage. In the charged exciton state, the two electrons have opposite spins (Fig. 1b) and the total electron spin is zero. For this reason, the electron-hole exchange interaction vanishes and no splitting is observed (Fig. 2; left).

Fig. 3 shows the polarization characteristics of the neutral and charged exciton resonances. At zero magnetic field, the two X^0 states are expected to couple to photons having orthogonal linear polarizations. The experimental results shown in Fig. 3a confirm the picture: the absorption resonances are sensitive only to photons with appropriate linear polarization. A magnetic field applied in the growth direction splits the X^{1-} transition into two lines separated by the Zeeman energy $E_z = g^* \mu_B B$, where

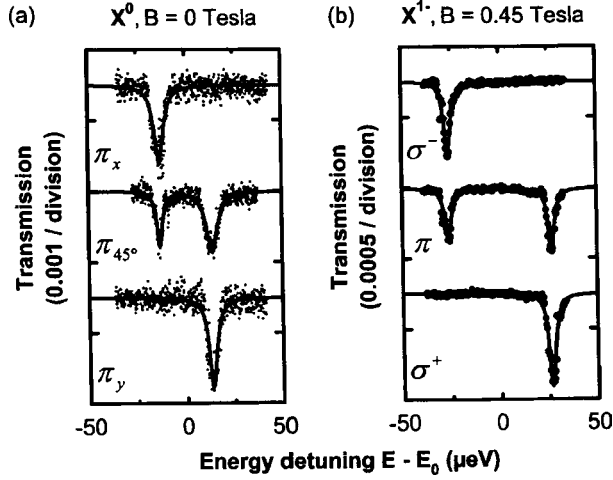


Fig. 3. Polarization dependence of the optical transitions in a single quantum dot* at 4.2 K. (a) Neutral exciton X^0 spectra for three different linear polarizations π_x , π_{45° and π_y at zero magnetic field, (b) Singly charged exciton X^{1-} spectra for left-hand circular polarization σ^- , linear polarization π and right-hand circular polarization σ^+ . The magnetic field was 0.45 T. In (a) and (b) the curves were offset vertically for clarity. *Note: Experimental data in Figs. 2, 3a, in 3b, 4 right and in Fig. 4 left were recorded on three different quantum dots.

g^* is the exciton g -factor and μ_B the Bohr magneton. In our sample, a typical value of g^* is -2 leading to a characteristic Zeeman splitting of $\sim 120 \mu\text{eV}/\text{T}^2$ [27]. Fig. 3b shows the polarization dependence of the two Zeeman split X^{1-} lines in a magnetic field of 0.45 T. For linear polarization π both resonances are active. Each transition can be addressed individually with circularly polarized light. The low and high energy branch were found to be sensitive to the orthogonal circular polarizations σ^- and σ^+ , respectively. This is anticipated for a negative exciton g -factor in agreement with earlier reports for similar samples [25,28]. For magnetic field higher than 6 T the σ^- resonance was strongly inhibited and σ^+ resonance became dominant [29].

As a consequence of the results described above, the optical polarization property of an individual QD can be controlled by the dc voltage applied between the top and the back electrode. For a given photon energy at zero magnetic field the QD's absorption within the voltage interval of the neutral exciton can be switched between the two orthogonal linear polarizations (Fig. 4; left). A small dc voltage is sufficient in order to switch in between the base vectors of the linear polarization. Furthermore, by applying a small magnetic field and thereby splitting the charged exciton into spin-polarized

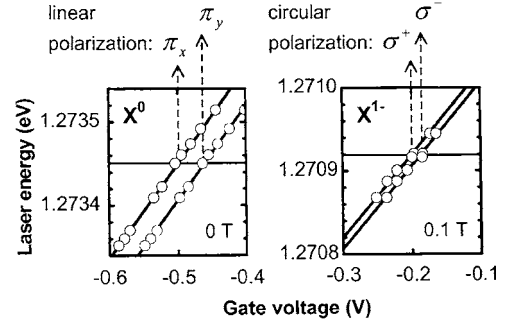


Fig. 4. Voltage control of polarization in a single quantum dot. Resonance energies of linearly polarized X^0 transitions at zero magnetic field (left) and circularly polarized X^{1-} transitions at 0.1 T (right) as function of gate voltage. The Zeeman splitting is $12 \mu\text{eV}$. The data were taken at 4.2 K.

Zeeman branches, orthogonal circular transitions are optically active in a single QD (Fig. 4; right). Again, a small voltage change is necessary in order to address the two orthogonal circular polarization states but to keep the resonance energy fixed. One should keep in mind, however, that charging the dot with a single electron shifts the resonance energy by 6 meV. The voltage-controlled polarization selection scheme is also valid for the photon emission, a very attractive application for QDs as a source of single photons with switchable polarization bases.

In summary, we have demonstrated that a self-assembled QD can be used to prepare excitonic states with an unprecedented degree of tunability. The tuning is achieved simply through a voltage. This property was demonstrated by applying high resolution laser spectroscopy to a single QD. Our results demonstrate that the electron-hole spin-exchange interaction can be switched off in a controlled way with gate voltage by adding a resident electron to a single QD through field effect. As a consequence of our results, the polarization of optical emission from a single QD can be switched between linear and circular polarization bases with dc voltage and a small applied magnetic field, an attractive feature for QDs in single photon source applications.

ACKNOWLEDGMENTS

Financial support for this work was provided in Germany by DFG grant no. SFB 631, in Switzerland by NCCR Quantum Photonics Grant No. 6993.1 and in the UK by the EPSRC.

REFERENCES

1. D. Loss and D. P. DiVincenzo, *Phys. Rev. A* **57**, 120 (1998).
2. G. Burkard, D. Loss, and D. P. DiVincenzo, *Phys. Rev. B* **59**, 2070 (1999).
3. A. Imamoğlu, D. D. Awschalom, G. Burkard, D. P. DiVincenzo, D. Loss, M. Sherwin, and A. Small, *Phys. Rev. Lett.* **83**, 4240 (1999).
4. P. Chen, C. Piermarocchi, and L. J. Sham, *Phys. Rev. Lett.* **87**, 067401 (2001).
5. E. Biolatti, R. C. Lotti, P. Zanardi, and F. Rossi, *Phys. Rev. Lett.* **85**, 5647 (2000).
6. D. Gammon, E. S. Snow, B. V. Shanabrook, D. S. Katzer, and D. Park, *Phys. Rev. Lett.* **76**, 3005 (1996).
7. J. R. Guest, T. H. Stievater, X. Li, J. Cheng, D. G. Steel, D. Gammon, D. S. Katzer, D. Park, C. Ell, A. Thränhardt, G. Khitrova, and H. M. Gibbs, *Phys. Rev. B* **65**, 241310 (2002).
8. T. H. Stievater, X. Li, J. R. Guest, D. G. Steel, D. Gammon, D. S. Katzer, and D. Park, *Appl. Phys. Lett.* **80**, 1876 (2002).
9. X. Li, Y. Wu, D. Steel, D. Gammon, T. H. Stievater, D. S. Katzer, D. Park, C. Piermarocchi, and L. J. Sham, *Science* **301**, 809 (2003).
10. P. Michler, A. Kiraz, C. Becher, W. V. Schoenfeld, P. M. Petroff, L. Zhang, E. Hu, and A. Imamoğlu, *Science* **290**, 2282 (2000).
11. E. Moreau, I. Robert, L. Manin, V. Thierry-Mieg, J. M. Gérard, I. Abram, *Phys. Rev. Lett.* **87**, 1836011 (2001).
12. Z. Yuan, B. E. Kardynal, R. M. Stevenson, A. J. Shields, C. J. Lobo, K. Cooper, N. S. Beattie, D. A. Ritchie, and M. Pepper, *Science* **295**, 102 (2001).
13. C. Santori, D. Fattal, J. Vučković, G. S. Solomon, and Y. Yamamoto, *Nature (London)* **419**, 594 (2002).
14. M. Pelton, C. Santori, J. Vučković, B. Zhang, G. S. Solomon, J. Plant, and Y. Yamamoto, *Phys. Rev. Lett.* **89**, 233602 (2002).
15. A. Högele, B. Alén, F. Bickel, R. J. Warburton, P. M. Petroff, and K. Karrai, *Physica E* **21**, 175 (2004).
16. A. Högele, S. Seidl, M. Kroner, R. J. Warburton, K. Karrai, B. D. Gerardot, and P. M. Petroff, *Phys. Rev. Lett.* **93**, 217401 (2004).
17. B. Alén, F. Bickel, K. Karrai, R. J. Warburton, and P. M. Petroff, *Appl. Phys. Lett.* **83**, 2235 (2003).
18. H. Drexler, D. Leonard, W. Hansen, J. P. Kotthaus, and P. M. Petroff, *Phys. Rev. Lett.* **73**, 2252 (1994).
19. J. M. Garcia, G. Medeiros-Ribeiro, K. Schmidt, T. Ngo, J. L. Feng, A. Lorke, J. P. Kotthaus, and P. M. Petroff, *Appl. Phys. Lett.* **71**, 2014 (1997).
20. R. J. Warburton, C. Schäfflein, D. Haft, A. Lorke, K. Karrai, J. M. Garcia, W. Schoenfeld, and P. M. Petroff, *Nature (London)* **405**, 926 (2000).
21. K. Karrai, R. J. Warburton, C. Schulhauser, A. Högele, B. Urbaszeck, E. J. McGhee, A. O. Govorov, J. M. Garcia, B. D. Gerardot, and P. M. Petroff, *Nature (London)* **427**, 135 (2004).
22. R. J. Warburton, C. Schulhauser, D. Haft, C. Schäfflein, K. Karrai, J. M. Garcia, W. Schoenfeld, and P. M. Petroff, *Phys. Rev. B* **65**, 113303 (2002).
23. D. Gammon, E. S. Snow, B. V. Shanabrook, D. S. Katzer, and D. Park, *Phys. Rev. Lett.* **76**, 3005 (1996).
24. G. Bester, S. Nair, and A. Zunger, *Phys. Rev. B* **67**, 161306 (2003).
25. M. Bayer, A. Kuther, A. Forchel, A. Gorbunov, V. B. Timofeev, F. Schäfer, J. P. Reithmaier, T. L. Reinecke, and S. N. Walck, *Phys. Rev. Lett.* **82**, 1748 (1999).
26. W. Langbein, P. Borri, U. Woggon, V. Stavarache, D. Reuter, and A. D. Wieck, *Phys. Rev. B* **69**, 161301 (2004).
27. C. Schulhauser, D. Haft, R. J. Warburton, K. Karrai, A. O. Govorov, A. V. Kalameitsev, A. Chaplik, W. Schoenfeld, J. M. Garcia, and P. M. Petroff, *Phys. Rev. B* **66**, 193303 (2002).
28. M. Bayer, G. Ortner, O. Stern, A. Kuther, A. A. Gorbunov, A. Forchel, P. Hawrylak, S. Fafard, K. Hinzer, T. L. Reinecke, S. N. Walck, J. P. Reithmaier, F. Klopff, and F. Schäfer, *Phys. Rev. B* **65**, 195315 (2002).
29. A. Högele, M. Kroner, S. Seidl, K. Karrai, M. Atatüre, J. Dreiser, A. Imamoğlu, R. J. Warburton, B. D. Gerardot, and P. M. Petroff, cond-mat/0410506, to appear in *Appl. Phys. Lett.* (2004).